Unsteady MHD Rear Stagnation-Point Flow of a Hybrid Nanofluid with Heat Generation/Absorption Effect

Nurul Amira Zainal[1,2], Kohilavani Naganthran[1], Roslinda Nazar[1,*]

[1] Department of Mathematical Sciences, Faculty of Science & Technology, Universiti Kebangsaan Malaysia, 43600 UKM Bangi, Selangor, Malaysia
[2] Fakulti Teknologi Kejuruteraan Mekanikal dan Pembuatan, Universiti Teknikal Malaysia Melaka, Hang Tuah Jaya, 76100 Durian Tunggal, Melaka, Malaysia

ARTICLE INFO	ABSTRACT
	The study of unsteady flow is essential in various engineering systems, for instance, the periodic fluid motion and start-up process. Therefore, this numerical study focuses on examining the unsteady magnetohydrodynamics (MHD) rear stagnation-point flow in Al_2O_3-Cu/H_2O hybrid nanofluid past a permeable stretching/shrinking surface with the impact of heat generation/absorption. By choosing a suitable similarity transformation, partial differential equations are transformed into a system of nonlinear ordinary differential equations and solved using the bvp4c function in the MATLAB package. The effects of the solution domain's operating parameters are analyzed, and dual solutions are observable as the sheet shrinks. It is found that the addition of the suction parameter escalates the heat transfer efficiency. Eventually, the existence of the unsteadiness parameter and the heat generation/absorption effect significantly encourage heat transfer deterioration.

1. Introduction

In producing better heat transfer mechanisms, hybrid nanofluids, which comprehend a homogeneous suspension of more than one nanoparticle possessing chemical and physical bonds, opens up another arena. The essential idea of this new form of nanofluid is to acquire development in heat transfer, thermophysical and hydrodynamic properties because of their potential role in many thermal applications, including fuel cells, hybrid-powered engines, and pharmaceutical processes [1-3].

Recently, multiple scientific experiments and numerical studies on hybrid nanofluid have been conducted. Jana *et al.,* [4] pioneered the investigation toward the thermal conductivity of several types of nanomaterial, including mono and hybrid nanomaterials. The study revealed that the nanofluid stability was directly affected by the properties of nanoparticles. Meanwhile, Turcu *et al.,* [5] were among the first to document the synthesis and characterisation of hybrid nanocomposite particle. However, it is reported that the thermal conductivity of the single nanoparticles shows

---

* *Corresponding author.*
E-mail address: rmn@ukm.edu.my

higher values in comparison with the hybrid nanocomposite particles due to the nanoparticle's compatibility effect. Nevertheless, Selvakumar and Suresh [6] demonstrated that the convective heat transfer coefficient in electronic heat sink is improved dramatically when Al_2O_3-Cu/H_2O is operated as the working fluid. An earlier study of the heat transfer enhancement in hybrid nanofluid using numerical analysis was conducted by Balla *et al.,* [7]. In another study, Takabi and Salehi [8] found out that the use of hybrid nanofluid increases the heat transfer efficiency, resulting in improved cooling efficiency and lower heated surface temperature. Since then, the study of nanofluid and hybrid nanofluid has attracted interest from many researchers considering various effects [9-17].

Previous investigations implied that the study of stagnation point flow plays an important role in several industrial and technological processes such as extrusion activity and polymer industry [18-20]. The classic problem of stagnation point in two-dimensional flow are related to Hiemenz [21] and Homann [22]. Meanwhile, the development of the boundary layer rear stagnation point at three-dimensional flow was established by Howarth [23-24], who extended the interesting work of Proudman and Johnson [25] and Robins and Howarth [26]. Later, the MHD impact in the unsteady rear stagnation point was tackled by Katagiri [27]. Turkyilmazoglu *et al.,* [28] performed the unsteady MHD rear stagnation point in the permeable and deformable sheet, and it is reported that the inclusion of unsteadiness and magnetic parameters consequently reduced the thickness of the boundary layer. In actual applications, the magnetic field plays an important role in rearranging the field of flow. The study of MHD in boundary layer flow is very important in the industry since its demand has continued in diverse fields of science, for instance, metallurgical procedures and petroleum production [29]. Some researches that implemented nanofluid and hybrid nanofluid as working fluid to test the effect of MHD can be reviewed in the studies by Zainal *et al.,* [30-31], Abdel-Nour *et al.,* [32], Armaghani *et al.,* [33], and Ishak *et al.,* [34].

To the best of the authors' knowledge, the study of rear stagnation-point flow still lacks intense investigation. Hence, the purpose of this current study is to examine the unsteady MHD rear stagnation point flow in Al_2O_3-Cu/H_2O hybrid nanofluid with heat generation/absorption influences. The governing equations are converted into an ordinary differential equations system on the basis of the corresponding transformation. The equation scheme is then numerically explained via the boundary value problem solver (bvp4c) in the MATLAB program. The generated results are significantly in accordance with previous literature. This analysis is original, and all the collected numerical results are authentic.

2. Mathematical Formulation

Consider an unsteady two-dimensional rear stagnation-point flow and heat transfer of Al_2O_3-Cu/H_2O hybrid nanofluid with magnetic effect past a permeable sheet as demonstrated in Figure 1. Note that the $x-$ axis moves opposite to the free-stream direction and is perpendicular to the $y-$ axis. It is assumed that the free-stream velocity is given by $u_\infty = -u_0 x/(1-\beta t)$, where u_0 and β is a real number and a constant that calculate the unsteadiness strength, respectively. Also, the wall has a moving velocity along the $x-$ axis with $u_w = u_0 x \lambda/(1-\beta t)$, and the wall transpiration velocity in the $y-$ axis is given by $v_w(x,t)$. Further, the wall temperature, T_w as well as the ambient temperature, T_∞ are considered constant. The hybrid nanofluid is utilised in this study provided that the effect of the agglomeration of nanoparticles on the thermophysical properties is ignored since the nanofluids are assumed to be synthesised as a steady combination. In addition, the size of the nanoparticles is considered to be uniform. Now, by using the standard approximations of the boundary layer, we have [31-35]

$$\frac{\partial u}{\partial x} + \frac{\partial v}{\partial y} = 0, \tag{1}$$

$$\frac{\partial u}{\partial t} + u\frac{\partial u}{\partial x} + v\frac{\partial u}{\partial y} = u_\infty \frac{du_\infty}{dx} + \frac{\mu_{hnf}}{\rho_{hnf}}\frac{\partial^2 u}{\partial y^2} - \frac{\sigma_{hnf}}{\rho_{hnf}}B_0^2\left(u - u_\infty\right), \tag{2}$$

$$\frac{\partial T}{\partial t} + u\frac{\partial T}{\partial x} + v\frac{\partial T}{\partial y} = \frac{k_{hnf}}{\left(\rho C_p\right)k_{hnf}}\frac{\partial^2 T}{\partial y^2} + \frac{Q}{\rho C_p}, \tag{3}$$

and the boundary conditions are:

$$v = v_w\left(x,t\right), u = u_w\left(x,t\right), T = T_w\left(x,t\right), \quad \text{at } y = 0,$$
$$u \to u_\infty\left(x,t\right), T \to T_\infty\left(x,t\right), \quad \text{as } y \to \infty. \tag{4}$$

The velocity components along the x and y axes are denoted by u and v, respectively, $v_w(x,t)$ is the velocity of the wall mass transfer, ρ_{hnf} is the density, μ_{hnf} is the dynamic viscosity, and B_0 is the transverse magnetic field. Further, k_{hnf} is the thermal conductivity, $\left(\rho C_p\right)_{hnf}$ is the heat capacity and Q is the heat generation/absorption coefficient. The considered thermophysical properties of the operating fluid are given in Table 1 [36]. While the correlation coefficient for the hybrid nanofluid is depicted in Table 2 [8-37].
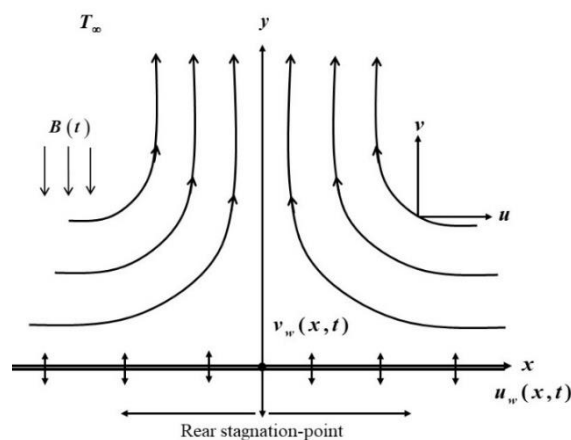
Fig. 1. Description of the physical model

Table 1
The H_2O, Al_2O_3 and Cu thermophysical properties

Physical properties	H_2O	Al_2O_3	Cu
$\rho\,(kg/m^3)$	997.1	3970	8933
$C_p\,(J/kgK)$	4179	765	385
$k\,(W/mK)$	0.613	40	400

Table 2
The alumina-copper/water (Al_2O_3-Cu/H_2O) correlation coefficient

Properties	Al_2O_3-Cu/H_2O
Density	$\rho_{hnf} = \left(1 - \phi_{hnf}\right)\rho_f + \phi_1 \rho_{s1} + \phi_2 \rho_{s2}$
Thermal capacity	$\left(\rho C_p\right)_{hnf} = \left(1 - \phi_{hnf}\right)\left(\rho C_p\right)_f + \phi_1 \left(\rho C_p\right)_{s1} + \phi_2 \left(\rho C_p\right)_{s2}$
Dynamic viscosity	$\mu_{hnf} = 1 \big/ \left(1 - \phi_{hnf}\right)^{2.5}$
Thermal conductivity	$\dfrac{k_{hnf}}{k_f} = \left[\dfrac{\left(\dfrac{\phi_1 k_{s1} + \phi_2 k_{s2}}{\phi_{hnf}}\right) + 2k_f + 2\left(\phi_1 k_{s1} + \phi_2 k_{s2}\right) - 2\phi_{hnf} k_f}{\left(\dfrac{\phi_1 k_{s1} + \phi_2 k_{s2}}{\phi_{hnf}}\right) + 2k_f - \left(\phi_1 k_{s1} + \phi_2 k_{s2}\right) + \phi_{hnf} k_f} \right]$

Thus, the following similarity variables are implemented [28-38]:

$$\psi\left(x, y, t\right) = \sqrt{\frac{u_0 v_f}{\left(1 - \beta t\right)}}\, x f\left(\eta\right), \quad \eta = \sqrt{\frac{u_0}{\left(1 - \beta t\right) v_f}}\, y, \quad \theta\left(\eta\right) = \frac{T - T_\infty}{T_w - T_\infty}, \tag{5}$$

$$u = \frac{u_0 x f'\left(\eta\right)}{\left(1 - \beta t\right)}, \quad v = -\sqrt{\frac{u_0 v_f}{\left(1 - \beta t\right)}}\, f\left(\eta\right), \quad v_w = -\sqrt{\frac{u_0 v_f}{\left(1 - \beta t\right)}}\, S, \tag{6}$$

where S is the constant mass flux parameter and v_f is the kinematic viscosity. Referring to the similarity variables, Eq. (5) and Eq. (6), Eq. (2) to Eq. (3) are converted into the ordinary differential equations, as such

$$\frac{\mu_{hnf}/\mu_f}{\rho_{hnf}/\rho_f}\, f''' + f f'' - f'^2 + 1 - \varepsilon\left(f' + \frac{\eta}{2} f'' + 1\right) - \frac{\sigma_{hnf}/\sigma_f}{\rho_{hnf}/\rho_f} M\left(f' + 1\right) = 0, \tag{7}$$

$$\frac{1}{\Pr} \frac{k_{hnf}/k_f}{\left(\rho C_p\right)_{hnf}\big/\left(\rho C_p\right)_f}\, \theta'' + f\theta' - f'\theta - \varepsilon\left(\theta + \frac{\eta}{2}\theta'\right) + \delta\theta = 0, \tag{8}$$

along with

$$f\left(0\right) = S,\ f'\left(0\right) = \lambda,\ \theta\left(0\right) = 1,$$
$$f'\left(\eta\right) \to -1,\ \theta\left(\eta\right) \to 0, \tag{9}$$

where $M = \sigma_f B / u_0 \rho_f$ is the magnetic coefficient with $B = B_0 \sqrt{1 - \beta t}$, $\Pr = \mu_f C_p / k_f$ is the Prandtl number, ε represents the unsteadiness parameter, and δ is the heat generation/absorption coefficient.

The physical quantities of concern are $Nu_x = \dfrac{xk_{hnf}}{k_f (T_w - T_\infty)} \left(-\dfrac{\partial T}{\partial y} \right)_{y=0}$, which is the local Nusselt

number and $C_f = \dfrac{\mu_{hnf}}{\rho_f u_\infty^2} \left(\dfrac{\partial u}{\partial y} \right)_{y=0}$ is the skin friction coefficient. Using the above-mentioned

information, finally, we obtain:

$$\text{Re}_x^{1/2} C_f = \frac{\mu_{hnf}}{\mu_f} f''(0), \quad \text{Re}_x^{-1/2} Nu_x = -\frac{k_{hnf}}{k_f} \theta'(0), \tag{10}$$

where $\text{Re}_x = u_0 x^2 / v_f$.

In this study, the bvp4c function in the MATLAB system is implemented to solve the resulting nonlinear ordinary differential equations. The bvp4c function is a finite difference code that performs the three stages of the Lobatto IIIa formula. This collocation polynomial provides a C1–continuous solution, which is uniformly accurate in the fourth-order interval at which the function is integrated. For the bvp4c solver's execution, the similarity equations in Eq. (7) and Eq. (8) along with the boundary conditions (9) are first converted into the following codes

$$y(1) = f, \; y(2) = f', \; y(3) = f'', \; y(4) = \theta, \; y(5) = \theta'. \tag{11}$$

Hence, Eq. (7) and Eq. (8) become

$$f''' = -\frac{\rho_{hnf}/\rho_f}{\mu_{hnf}/\mu_f} \left[ff'' - f'^2 + 1 - \varepsilon \left(f' + \frac{\eta}{2} f'' + 1 \right) - \frac{\sigma_{hnf}/\sigma_f}{\rho_{hnf}/\rho_f} M (f' + 1) \right], \tag{12}$$

$$\theta'' = -\text{Pr} \frac{(\rho C_p)_{hnf}/(\rho C_p)_f}{k_{hnf}/k_f} \left[f\theta' - f'\theta - \varepsilon \left(\theta + \frac{\eta}{2} \theta' \right) + \delta\theta \right], \tag{13}$$

whereas the code for boundary condition is disclosed as

$$ya(1) - S, \; ya(2) - \lambda, \; ya(4) - 1, \; yb(2) + 1, \; yb(4). \tag{14}$$

At this point, ya is the condition at $\eta = 0$ and yb is the condition at $\eta = \infty$. The bvp4c function is executed using an appropriate value of the governing parameters with the relevant boundary layer thickness η_∞ until the convergence criteria is accomplished.

3. Results Interpretation

The bvp4c solver in MATLAB programming is used to elucidate the resulting nonlinear ordinary differential equations presented in Eq. (7) to Eq. (8) in common with the boundary conditions (9). The expressed boundary value problem is demoted to the ordinary differential equations system of the first-order, initially. The bvp4c method is a prominent coder exercised by countless investigators to demonstrate the boundary value query. A preliminary forecast of the primary mesh point and the step size of variations is important for the necessary solutions guarantee. The necessary

approximation of boundary layer thickness is vital during an effort to discover more than one solution. The users also need to provide several trials in supplying an excellent preliminary guess before a necessary result is obtained. The reliability of the findings is measured with Turkyilmazoglu *et al.,* [28] and Bhattacharyya [39], as accessible in Table 3. The authors specifically found that the current results conform to the previous work remarkably. Hence, we believe that the intended computational model can be completely applied to determine dynamic fluid flow activity with substantial confidence.

Table 3
Approximation values of $\mathrm{Re}_x^{1/2} C_f$ by certain values of λ when $\varepsilon = M = \delta = S = \phi_1 = \phi_2 = 0$

λ	Present result		Turkyilmazoglu *et al.,* [28]		Bhattacharyya [39]	
	First solution	First solution	First solution	Second solution	First solution	Second solution
-0.25	1.4022408	-	1.4022408	-	1.4022405	-
-0.50	1.4956698	-	1.4956670	-	1.4956697	-
-0.75	1.4892982	-	1.4892982	-	1.4892981	-
-1.00	1.3288169	0.0000000	1.3288168	0.0000000	1.3288169	0.0000000
-1.15	1.0822312	0.1167021	1.0822312	0.1167021	1.0822316	0.1167023
-1.20	0.9324733	0.2336497	0.9324733	0.2336497	0.9324728	0.2336491
-1.2465	0.5842817	0.5542962	0.5842813	0.5542947	0.5842915	0.5542856
-1.24657	0.5745257	0.5640125	0.5774525	0.5640081	0.5745268	0.5639987

The preparation of compatible conventional/hybrid nanofluids is the crucial element for measuring nanofluids' flow behaviour and the efficiency of heat transfer. The Al_2O_3-Cu/H_2O hybrid nanofluid is selected as the working fluid because of the outstanding work of Suresh *et al.,* [40] in developing an exploration practice to scrutinise the Al_2O_3-Cu/H_2O thermophysical properties. In another study, Suresh *et al.,* [41] performed the synthesis of Al_2O_3-Cu/H_2O nanocomposite powder and its characteristics for various volume concentrations. In their noteworthy findings, nanofluid stability is observed to decrease as volume concentration increases. Further, according to Arifin *et al.,* [42], the development of stable nanofluids was to optimise the thermal properties of operating fluids with the minimal use of nanoparticles. In this study, a distinct set of values for ϕ_2 is implemented $(0.00 \leq \phi_2 \leq 0.02)$, while ϕ_1 is fixed at 0.01. On another point, different values of the limiting parameters are defined to the preceding scope; $-2.0 \leq \varepsilon \leq -6.0$, $5.0 \leq S \leq 7.0$, and $0.5 \leq \delta \leq 2.5$ ensure the consistency of the solutions obtained. Since there is no experimental evidence exist, the choice of parameter values was determined by the values selected from previous researchers to ensure the establishment of the dual solutions [28]. Meanwhile, the range values for $\phi_1 = 0.01$, and $0.00 \leq \phi_2 \leq 0.02$ in this study is selected based on the experimental work done by Suresh *et al.,* [41], who conducted the synthesis, characterisation of Al_2O_3-Cu/water nanocomposite powder for different volume concentrations 0.1%, 0.33%, 0.75%, 1%, and 2%. In his valuable study, the stability of the prepared nanofluids was determined by measuring the pH of the nanofluids and the nanofluid stability was found to diminish with increasing volume concentration. The values of $M = 6.0$ is used based on the work done by Turkyilmazoglu *et al.,* [28] to ensure the existence of the dual solution while $\mathrm{Pr} = 6.2$ is implemented so that the results are compatible with the water-based nanofluid [11-12].

The bvp4c function in the MATLAB programming is utilised in this research work to solve the governing Eq. (7) and Eq. (8) along with the boundary conditions (9). The above-proposed approach is a significant technique for tackling the boundary value issues that were thoroughly defined by numerous scholars. In order to accomplish the necessary solution, a suitable preliminary estimation

and the boundary layer thickness, η_∞ shall be appointed according to the values of the mentioned parameter. Generally, this analysis aims to investigate the input parameter impact, including the unsteadiness parameter (ε), the suction parameter (S), and the heat generation/absorption parameter (δ) over the physical quantities of interest. The present research also focused on identifying more than one solution which exists in the system of equations. From the generated results, the non-uniqueness (dual) solutions are perceived to a particular range of λ_c, reflecting the meeting point of dual solutions or referred to a critical point. It is noticed that the dual solutions are seen in Figure 2 to Figure 9 as the sheet shrinks $(\lambda < 0)$, while only a single solution can be noticed as the sheet stretches $(\lambda > 0)$.

The influence of ε is presented in Figure 2 to Figure 5. The skin friction coefficient $(f''(0))$ of Al_2O_3-Cu/H_2O hybrid nanofluid $(\phi_1 = \phi_2 = 0.01)$ past a shrinking surface along with the heat transfer rate $(-\theta'(0))$ is accessible in Figure 2 and Figure 3. Figure 2 establishes that the reduction in ε worsens $f''(0)$, meanwhile, the addition of ε triggers the viscosity of the working fluid to accelerate whilst the sheet is shrinking. This essentially increases the velocity of the fluid past the shrinking surface, as seen in Figure 4. The profile of velocity, $f'(\eta)$ (see Figure 4) discloses that the thickness of the momentum boundary layer is decreased proportionally to the ε. This enhances the velocity gradient as the fluid density increases. As $f''(0)$ declines, the finding indicates that the frictional drag applied on the unsteady Al_2O_3-Cu/H_2O hybrid nanofluid flow is declined toward the shrinking sheet, which can restrict separation of the boundary layer flow. In the meantime, Figure 3 illustrates a declining trend of $-\theta'(0)$ when the values of ε decreases in both solutions, and this indicates that the heat transfer efficiency decreases in Al_2O_3-Cu/H_2O hybrid nanofluid. This discovery helps to defend the fact that the appearance of ε hypothetically reduces the heat transfer performance in Al_2O_3-Cu/H_2O hybrid nanofluid. On the other note, the temperature profiles $\theta(\eta)$ in Figure 5 demonstrates the reduction in the temperature of Al_2O_3-Cu/H_2O hybrid nanofluid. The decrease in the temperature of hybrid nanofluid lessens the conductivity of heat. We understand that the occurrence of unsteady flow and the adoption of assorted parameters may trigger this behaviour. The unsteady parameter may enforce any sum of heat flow in the regulating framework, ultimately aggravating the heat transfer mechanism. Overall, both profiles, i.e., $f'(\eta)$ and $\theta(\eta)$, asymptotically fulfilled the far-field boundary conditions (9) when $\eta_\infty = 6$ is executed.

Fig. 2. $f''(0)$ against λ by various ε

Fig. 3. $-\theta'(0)$ against λ by various ε

Penerbit
Akademia Baru
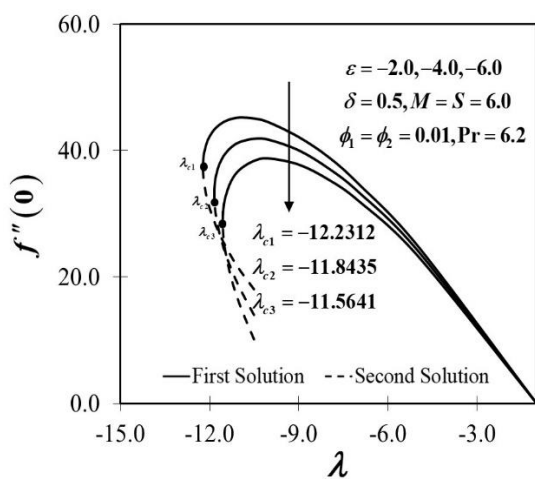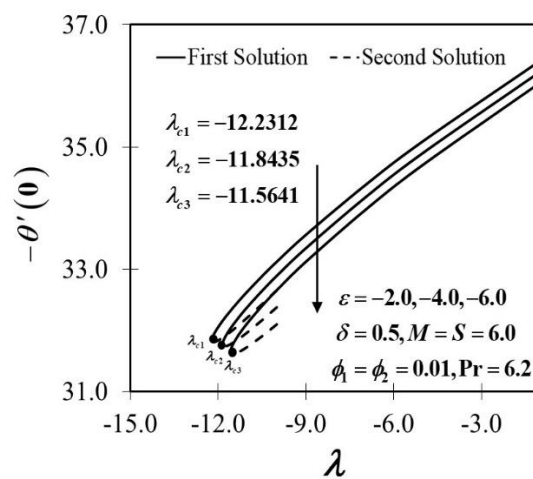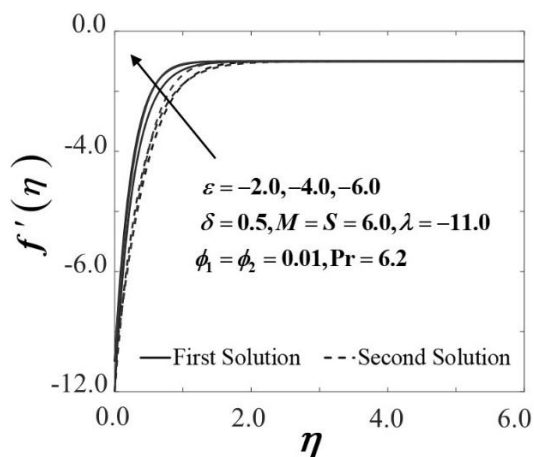
Fig. 4. $f'(\eta)$ with $\lambda = -11.0$
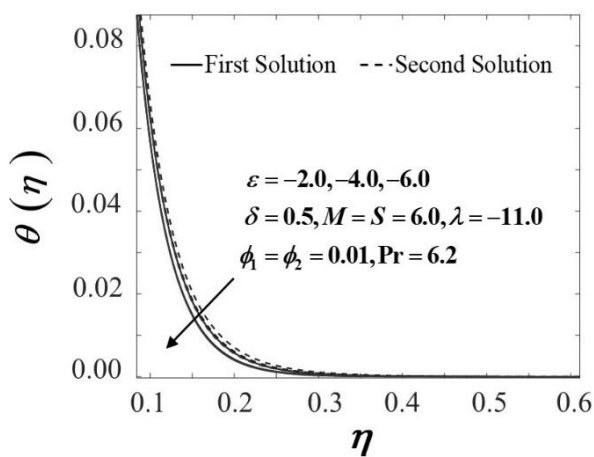
Fig. 5. $\theta(\eta)$ with $\lambda = -11.0$

Figure 6 and Figure 7 demonstrate the impact of S toward λ as the suction values are varied. The hybrid Al₂O₃-Cu/H₂O nanofluid behaviour is depicted in Figure 6 concerning the skin friction coefficient, $f''(0)$ as the sheet shrinks. Figure 6 captures that both solutions depicted an improvement in $f''(0)$ as S increased. The existence of suction on a permeable surface will potentially promote stabilisation of the boundary layer. Also, the suction reduces the pressure on the bodies, thereby magnifying the velocity gradient. Moreover, according to the generated results in Figure 7, $-\theta'(0)$ is amplified in the first and second solution, which is proportional to the rate of heat transfer when S increases. Realise that the suction effect permits Al₂O₃–Cu/H₂O hybrid nanofluid molecules to occupy the surface and then physically improve the heat transfer rate at the permeable surface. From the current and existing evidence, the authors may conclude that the suction parameter greatly facilitates heat transfer improvement.
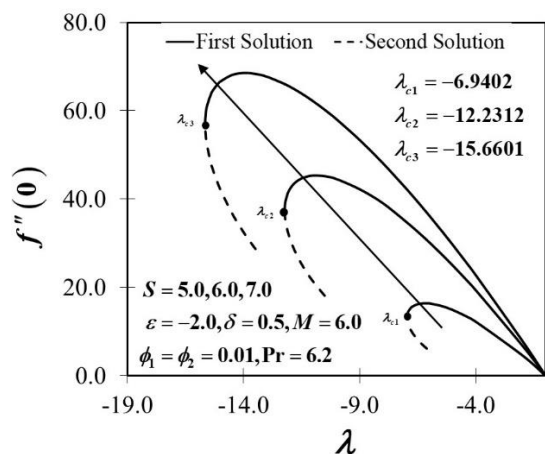
Fig. 6. $f''(0)$ against λ by various S
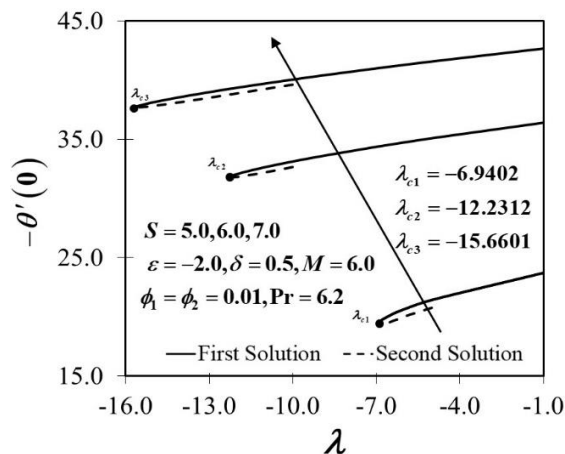
Fig. 7. $-\theta'(0)$ against λ by various S

Figure 8 and Figure 9 are prepared to reveal the effect of δ in relation to λ when $\delta = 0.5, 1.5, 2.5$ which represents the heat generation influences toward the shrinking surface. Figure 8 highlights that as δ increase, $-\theta'(0)$ decreases in Al₂O₃–Cu/H₂O hybrid nanofluid. Physically, the additional heat provided to the Al₂O₃–Cu/H₂O hybrid nanofluid triggers temperature to rise, thereby reducing the efficiency of heat transfer. On the other note, the temperature profiles $\theta(\eta)$ in Figure 9 support the trend seen in Figure 8, which demonstrates the changes in temperature of the Al₂O₃–Cu/H₂O

hybrid nanofluid. The increase in the heat generation parameter allows the thermal layer thickness and thermal gradient to increase because energy is generated at the thermal boundary layer.
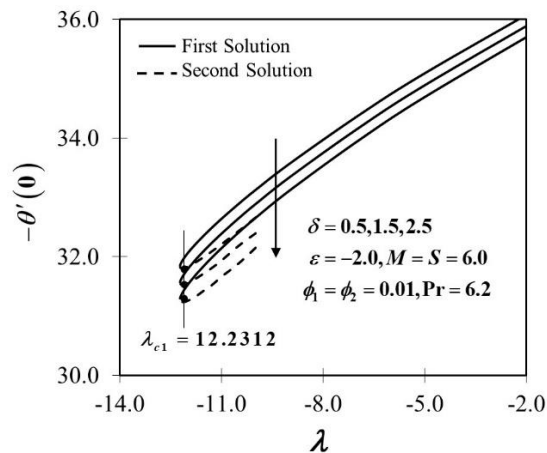
Fig. 8. $-\theta'(0)$ with $\delta = 0.5, 1.5, 2.5$
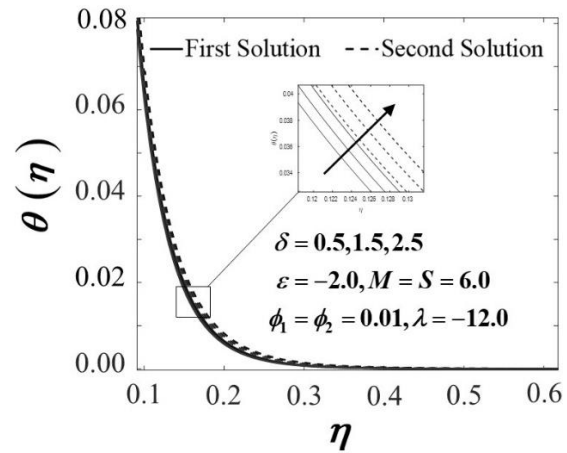
Fig. 9. $\theta(\eta)$ with $\delta = 0.5, 1.5, 2.5$

4. Conclusion

The current study reflects the impact of suction and unsteadiness parameters in Al_2O_3–Cu/H_2O hybrid nanofluid with heat generation/absorption. The numerical results for the skin friction coefficient and the local Nusselt number are deduced with the aid of bvp4c features in the MATLAB package. A decrease in the unsteadiness parameter reduces the skin friction coefficient over the shrinking permeable sheet. The findings of the local Nusselt number suggest that the unsteadiness parameter greatly facilitates the degradation of heat transfer. Further, the rise in the suction parameter encourages stabilisation of the boundary layer and increases thermal efficiency as well. The inclusion of heat generation/absorption in the operating fluid generates a greater temperature profile, which reduces the heat transfer performance.

References
[1] Minkowycz, W. J., E. Sparrow, and J. P. Abraham, eds. *Nanoparticle Heat Transfer and Fluid Flow*. Vol. 4. CRC Press, 2016. https://doi.org/10.1201/b12983
[2] Das, Sarit K., Stephen U. Choi, Wenhua Yu, and T. Pradeep. *Nanofluids: science and technology*. John Wiley & Sons, 2008. https://doi.org/10.1002/9780470180693
[3] Khashi'ie, Najiyah Safwa, Norihan Md Arifin, Ezad Hafidz Hafidzuddin, and Nadihah Wahi. "Thermally stratified flow of Cu-Al_2O_3/water hybrid nanofluid past a permeable stretching/shrinking circular cylinder." *Journal of Advanced Research in Fluid Mechanics and Thermal Sciences* 63, no. 1 (2019): 154-163.
[4] Jana, Soumen, Amin Salehi-Khojin, and Wei-Hong Zhong. "Enhancement of fluid thermal conductivity by the addition of single and hybrid nano-additives." *Thermochimica Acta* 462, no. 1-2 (2007): 45-55. https://doi.org/10.1016/j.tca.2007.06.009
[5] Turcu, R., A. L. Darabont, A. Nan, N. Aldea, D. Macovei, D. Bica, L. Vekas et al. "New polypyrrole-multiwall carbon nanotubes hybrid materials." *Journal of Optoelectronics and Advanced Materials* 8, no. 2 (2006): 643-647.
[6] Selvakumar, Ponnusamy, and Sivan Suresh. "Use of Al_2O_3-Cu/Water Hybrid Nanofluid in an Electronic Heat Sink." *IEEE Transactions on Components, Packaging, and Manufacturing Technology* 2, no. 9-10 (2012): 1600-1607. https://doi.org/10.1109/TCPMT.2012.2211018

[7]   Balla, Hyder H., Shahrir Abdullah, Wan MohdFaizal, Rozli Zulkifli, and Kamaruzaman Sopian. "Numerical study of the enhancement of heat transfer for hybrid CuO-Cu nanofluids flowing in a circular pipe." *Journal of Oleo Science* 62, no. 7 (2013): 533-539. https://doi.org/10.5650/jos.62.533

[8]   Takabi, Behrouz, and Saeed Salehi. "Augmentation of the heat transfer performance of a sinusoidal corrugated enclosure by employing hybrid nanofluid." *Advances in Mechanical Engineering* 6 (2014): 147059. https://doi.org/10.1155/2014/147059

[9]   Zainal, N. A., R. Nazar, K. Naganthran, and I. Pop. "Viscous dissipation and MHD hybrid nanofluid flow towards an exponentially stretching/shrinking surface." *Neural Computing and Applications* (2021): 1-11. https://doi.org/10.1007/s00521-020-05645-5

[10]   Khashi'ie, Najiyah Safwa, Norihan M. Arifin, John H. Merkin, Rusya Iryanti Yahaya, and Ioan Pop. "Mixed convective stagnation point flow of a hybrid nanofluid toward a vertical cylinder." *International Journal of Numerical Methods for Heat & Fluid Flow* (2021). https://doi.org/10.1108/HFF-11-2020-0725

[11]   Waini, Iskandar, Anuar Ishak, and Ioan Pop. "Flow Towards a Stagnation Region of a Vertical Plate in a Hybrid Nanofluid: Assisting and Opposing Flows." *Mathematics* 9, no. 4 (2021): 448. https://doi.org/10.3390/math9040448

[12]   Khashi'ie, Najiyah S., Norihan M. Arifin, Ioan Pop, and Nur S. Wahid. "Effect of suction on the stagnation point flow of hybrid nanofluid toward a permeable and vertical Riga plate." *Heat Transfer* 50, no. 2 (2021): 1895-1910. https://doi.org/10.1002/htj.21961

[13]   Bachok, Norfifah, Anuar Ishak, and Ioan Pop. "Mixed convection boundary layer flow near the stagnation point on a vertical surface embedded in a porous medium with anisotropy effect." *Transport in Porous Media* 82, no. 2 (2010): 363-373. https://doi.org/10.1007/s11242-009-9431-0

[14]   Bachok, Norfifah, Anuar Ishak, and Ioan Pop. "Stagnation point flow toward a stretching/shrinking sheet with a convective surface boundary condition." *Journal of the Franklin Institute* 350, no. 9 (2013): 2736-2744. https://doi.org/10.1016/j.jfranklin.2013.07.002

[15]   Bachok, Norfifah, and Anuar Ishak. "Mixed convection boundary layer flow over a permeable vertical cylinder with prescribed surface heat flux." *European Journal of Scientific Research* 34, no. 1 (2009): 46-54.

[16]   Salleh, Siti Nur Alwani, Norfifah Bachok, Norihan Md Arifin, Fadzilah Md Ali, and Ioan Pop. "Stability analysis of mixed convection flow towards a moving thin needle in nanofluid." *Applied Sci*ences 8, no. 6 (2018): 842. https://doi.org/10.3390/app8060842

[17]   Zokri, Syazwani Mohd, Nur Syamilah Arifin, Abdul Rahman Mohd Kasim, and Mohd Zuki Salleh. "Free Convection Boundary Layer Flow of Jeffrey Nanofluid on a Horizontal Circular Cylinder with Viscous Dissipation Effect." *Journal of Advanced Research in Micro and Nano Engineering* 1, no. 1 (2020): 1-14.

[18]   Rauwendaal, Chris. *Polymer extrusion*. Aufl. München: Hanser, 1985.

[19]   Fisher, Edwin George. *Extrusion of plastics*. Wiley, 1976.

[20]   Khashi'ie, Najiyah Safwa, Ezad Hafidz Hafidzuddin, Norihan Md Arifin, and Nadihah Wahi. "Stagnation point flow of hybrid nanofluid over a permeable vertical stretching/shrinking cylinder with thermal stratification effect." *CFD Letters* 12, no. 2 (2020): 80-94.

[21]   Hiemenz, Karl. "Die Grenzschicht an einem in den gleichformigen Flussigkeitsstrom eingetauchten geraden Kreiszylinder." *Dinglers Polytech. J.* 326 (1911): 321-324.

[22]   Homann, Fritz. "Der Einfluss grosser Zähigkeit bei der Strömung um den Zylinder und um die Kugel." *ZAMM-Journal of Applied Mathematics and Mechanics/Zeitschrift für Angewandte Mathematik und Mechanik* 16, no. 3 (1936): 153-164. https://doi.org/10.1002/zamm.19360160304

[23]   Howarth, J. A. "A note on boundary-layer growth at an axisymmetric rear stagnation point." *Journal of Fluid Mechanics* 59, no. 4 (1973): 769-773. https://doi.org/10.1017/S0022112073001850

[24]   Howarth, J. A. "Boundary-layer growth at a three-dimensional rear stagnation point." *Journal of Fluid Mechanics* 67, no. 2 (1975): 289-297. https://doi.org/10.1017/S0022112075000316

[25]   Proudman, Ian, and Kathleen Johnson. "Boundary-layer growth near a rear stagnation point." *Journal of Fluid Mechanics* 12, no. 2 (1962): 161-168. https://doi.org/10.1017/S0022112062000130

[26]   Robins, A. J., and J. A. Howarth. "Boundary-layer development at a two-dimensional rear stagnation point." *Journal of Fluid Mechanics* 56, no. 1 (1972): 161-171. https://doi.org/10.1017/S0022112072002241

[27]   Katagiri, Masakazu. "On the separation of magnetohydrodynamic flow near the rear stagnation point." *Journal of the Physical Society of Japan* 27, no. 4 (1969): 1045-1050. https://doi.org/10.1143/JPSJ.27.1045

[28]   Turkyilmazoglu, Mustafa, Kohilavani Naganthran, and Ioan Pop. "Unsteady MHD rear stagnation-point flow over off-centred deformable surfaces." *International Journal of Numerical Methods for Heat & Fluid Flow* 27, no. 7 (2017): 1554-1570. https://doi.org/10.1108/HFF-04-2016-0160

[29] Abel, M. Subhas, Jagadish V. Tawade, and Jyoti N. Shinde. "The effects of MHD flow and heat transfer for the UCM fluid over a stretching surface in presence of thermal radiation." *Advances in Mathematical Physics* 2012 (2012). https://doi.org/10.1155/2012/702681

[30] Zainal, Nurul Amira, Roslinda Nazar, Kohilavani Naganthran, and Ioan Pop. "Stability analysis of MHD hybrid nanofluid flow over a stretching/shrinking sheet with quadratic velocity." *Alexandria Engineering Journal* 60, no. 1 (2021): 915-926. https://doi.org/10.1016/j.aej.2020.10.020

[31] Zainal, Nurul Amira, Roslinda Nazar, Kohilavani Naganthran, and Ioan Pop. "Heat generation/absorption effect on MHD flow of hybrid nanofluid over bidirectional exponential stretching/shrinking sheet." *Chinese Journal of Physics* 69 (2021): 118-133. https://doi.org/10.1016/j.cjph.2020.12.002

[32] Abdel-Nour, Zaim, Abderrahmane Aissa, Fateh Mebarek-Oudina, A. M. Rashad, Hafiz Muhammad Ali, M. Sahnoun, and M. El Ganaoui. "Magnetohydrodynamic natural convection of hybrid nanofluid in a porous enclosure: numerical analysis of the entropy generation." *Journal of Thermal Analysis and Calorimetry* 141, no. 5 (2020): 1981-1992. https://doi.org/10.1007/s10973-020-09690-z

[33] Armaghani, T., M. S. Sadeghi, A. M. Rashad, M. A. Mansour, Ali J. Chamkha, A. S. Dogonchi, and Hossam A. Nabwey. "MHD mixed convection of localized heat source/sink in an Al_2O_3-Cu/water hybrid nanofluid in L-shaped cavity." *Alexandria Engineering Journal* 60, no. 3 (2021): 2947-2962. https://doi.org/10.1016/j.aej.2021.01.031

[34] Ishak, Anuar, Roslinda Nazar, Norfifah Bachok, and Ioan Pop. "MHD mixed convection flow adjacent to a vertical plate with prescribed surface temperature." *International Journal of Heat and Mass Transfer* 53, no. 21-22 (2010): 4506-4510. https://doi.org/10.1016/j.ijheatmasstransfer.2010.06.043

[35] Devi, S. Suriya Uma, and SP Anjali Devi. "Numerical investigation of three-dimensional hybrid Cu-Al_2O_3/water nanofluid flow over a stretching sheet with effecting Lorentz force subject to Newtonian heating." *Canadian Journal of Physics* 94, no. 5 (2016): 490-496. https://doi.org/10.1139/cjp-2015-0799

[36] Abu-Nada, Eiyad, and Hakan F. Oztop. "Effects of inclination angle on natural convection in enclosures filled with Cu-water nanofluid." *International Journal of Heat and Fluid Flow* 30, no. 4 (2009): 669-678. https://doi.org/10.1016/j.ijheatfluidflow.2009.02.001

[37] Ghalambaz, Mohammad, Natalia C. Roşca, Alin V. Roşca, and Ioan Pop. "Mixed convection and stability analysis of stagnation-point boundary layer flow and heat transfer of hybrid nanofluids over a vertical plate." *International Journal of Numerical Methods for Heat & Fluid Flow* 30, no. 7 (2019): 3737-3754. https://doi.org/10.1108/HFF-08-2019-0661

[38] Fang, Tiegang, and Wei Jing. "Closed-form analytical solutions of flow and heat transfer for an unsteady rear stagnation-point flow." *International Journal of Heat and Mass Transfer* 62 (2013): 55-62. https://doi.org/10.1016/j.ijheatmasstransfer.2013.02.049

[39] Bhattacharyya, Krishnendu. "Dual solutions in boundary layer stagnation-point flow and mass transfer with chemical reaction past a stretching/shrinking sheet." *International Communications in Heat and Mass Transfer* 38, no. 7 (2011): 917-922. https://doi.org/10.1016/j.icheatmasstransfer.2011.04.020

[40] Suresh, S., K. P. Venkitaraj, P. Selvakumar, and M. Chandrasekar. "Synthesis of Al_2O_3-Cu/water hybrid nanofluids using two step method and its thermo physical properties." *Colloids and Surfaces A: Physicochemical and Engineering Aspects* 388, no. 1-3 (2011): 41-48. https://doi.org/10.1016/j.colsurfa.2011.08.005

[41] Suresh, S., K. P. Venkitaraj, and P. Selvakumar. "Synthesis, Characterisation of Al_2O_3-Cu Nano composite powder and water based nanofluids." In *Advanced Materials Research*, vol. 328, pp. 1560-1567. Trans Tech Publications Ltd, 2011. https://doi.org/10.4028/www.scientific.net/AMR.328-330.1560

[42] Arifin, N. M., R. Nazar, and I. Pop. "Non-isobaric Marangoni boundary layer flow for Cu, Al_2O_3 and TiO_2 nanoparticles in a water based fluid." *Meccanica* 46, no. 4 (2011): 833-843. https://doi.org/10.1007/s11012-010-9344-6